J. Fluid Mech. (1995), *vol.* 296, *pp.* 353–372

The localization length of randomly scattered water waves

By ANDRÉ NACHBIN

Instituto de Matemática Pura e Aplicada, Estrada D. Castorina, 110, Rio de Janeiro, RJ, CEP 22460-320, Brazil † *and*

Department of Mathematics, Center for Applied Mathematics and Statistics, New Jersey Institute of Technology, Newark, NJ 07102, USA

(Received 19 July 1993 and in revised form 20 December 1994)

A theory for the reflection-transmission problem of linear water waves in shallow channels with large-amplitude, rapidly varying topographies is given in Nachbin & Papanicolaou (1992*b*). However, it is very difficult to extract quantitative information from the theory in the large-amplitude regime. In this work, theoretical parameters are evaluated numerically, through the use of a numerical Schwarz–Christoffel transformation and of a Monte Carlo simulation. This enables the theory to be applied to its full extent. As a result we calculate the localization length for any given type of random bottom topography. Additionally, the numerical conformal mapping provides further insight into depth effects arising from potential theory. Statistical results, for numerically generated reflected waves, are in very good agreement with the theory for both piecewise-linear and piecewise-constant topographies of large amplitude.

1. Introduction.

The interaction of surface gravity waves with a rough bottom topography has been analysed extensively in recent years. A wide range of experimental and theoretical research work have been reported, because of its importance in oceanography and in the development of new techniques for analysing scattering problems in fluid mechanics.

In the context of applications, submerged obstacles can provide different mechanisms for the protection of coastal regions. In the periodic case, the phenomenon of Bragg reflection is of primary interest (see for example Guazzelli, Rey & Belzons 1992 and references therein). For fully erodible beds, the Bragg resonance phenomenon may lead to the growth of new sandbars in the seaward direction (Guazzelli *et al.* 1992; O'Hare & Davies 1990 and references therein). Numerical experiments with periodic beds of large amplitude were performed by Dalrymple & Kirby (1986) using the boundary-element method.

When the bottom topography has an arbitrary rapidly varying profile we have the phenomenon of localization. This is typical of linear waves propagating in a one-dimensional random media. Localization means that the transmission coefficient of a plane wave decays exponentially as a function of the length of the rough segment of the channel. This apparent attenuation phenomenon arises from the disordered multiple scattering of waves, and provides another mechanism for coastal protection.

† Address for correspondence.

This has been observed in the laboratory experiments conducted by Belzons, Guazzelli & Parodi (1988).

A review of ocean waves in random media is given by Mysak (1978). In particular, Hasselmann (1966) used the formalism of quantum field theory to describe the scattering of internal and surface waves by topographic irregularities in a stratified fluid. Both wave amplitudes and bottom displacements are considered small so that perturbation techniques are applicable. Long (1973) used Hasselmann's (1966) theory in the homogeneous fluid case of surface waves alone and observed that the presence of a random topography could be sufficient to account for the swell decay, which was observed in the Joint North Sea Wave Project (JONSWAP). Long concludes that with the available data they were not able to prove that bottom scattering is the dominant process causing swell decay, but that the effect is of the right order. More details can be found in § 4.3.

More recently Devillard, Dunlop & Souillard (1988) considered the case of random piecewise-constant topographies and, by using a transfer matrix technique, estimated the localization length for time harmonic surface waves. They compare their results with the experiments of Belzons *et al.* (1988) and obtain good agreement over a band of wavenumbers. More details can be found in § 4.3.

In the present work we consider arbitrary rapidly varying topographies which implies

$$\frac{\text{typical wavelength}}{\text{typical length scale for bottom irregularities}} = \frac{1}{\varepsilon}.$$

We also assume the long-wave regime with

$$\frac{\text{typical depth}}{\text{typical wavelength}} = O(\varepsilon)$$

and linear theory with

$$\frac{\text{typical amplitude}}{\text{typical depth}} = O(\varepsilon),$$

for small ε. Using table 1.1 in Mei (1983) we have that a tsunami of period 10 minutes, propagating over the continental shelf (depth $\approx$ 200 m) with shallow water speed ($c = (gh)^{1/2} \approx 44.27$ m s^{-1}) is 26.8 km long. Note that waves of 1 km or longer are in the long-wave regime and therefore interact with the topography. Rapidly varying features of the topography range from hundreds of metres to the kilometre scale, and with an amplitude of say 20 m the motion can be described by linear theory. In this regime the bottom is modelled as a random process, and we fall into the extensively studied area of wave propagation in random media. A very broad source of references, for different physical applications, can be found in Asch *et al.* (1991) and in Gredeskul & Kivshar (1992).

To study water waves in random media Nachbin & Papanicolaou (1992*b*) developed a theory for the reflection-transmission problem, based on the asymptotic analysis of stochastic differential equations. This theory accounts for general bottom profiles of large amplitude and is not restricted to monochromatic waves. Pulse-shaped waves are also considered.

No mild-slope restrictions are required, nor does the profile need to be approximated by piecewise flat segments. The theory has its limitations based on the fact that the free surface disturbances are of infinitesimal amplitude (i.e. linear theory), the fluid is considered inviscid, the flow is irrotational and the bottom is rigid. We also assume that the waves are long because the scattering of short waves has a negligible overall

effect. This is supported by the work of Devillard *et al.* (1988) and will be discussed in more detail in §4.3. Moreover there is evidence that potential theory provides a good model for the reflection-transmission problems. Recently Rey, Belzons & Guazzelli (1992) performed experiments on the propagation of linear and weakly nonlinear gravity waves over a rectangular submerged bar. They examined the effects arising from the finite amplitude of the surface wave and those coming from the generation of vorticity around the sharp edges of the topography. They concluded that a rounded corner can suppress vortex shedding but also that the rectangular bar's corner has a small influence on the reflection coefficient as well as the wave amplitude over the bed. In conclusion, their study showed that weak nonlinearity and weak vorticity have only a small effect on the reflection coefficient results, which are in good agreement with linear potential theory.

The results presented in Rey *et al.* (1992) support the use of potential theory to study the interaction between gravity waves and rough topographies, as well as to obtain estimates of the wave's penetration depth into the random medium. The length scale related to the penetration depth is called the localization length.

In Nachbin & Papanicolaou (1992*b*) numerical experiments were carried out in order to validate the asymptotic theory developed. Even though the theory is valid for $O(1)$ depth variations, the results exhibited took into account only cases of topographies of moderate amplitude. When the amplitudes are large it is very difficult to extract quantitative information from the expressions provided by the theory.

In this work we present an algorithm for calculating the effective parameter for scattering and the localization length defined in Nachbin & Papanicoloau (1992*b*). The numerical method is designed to accommodate arbitrary topography profiles, with no restriction on the amplitude nor on its smoothness. New numerical experiments are performed to show the wide range of validity of the stochastic theory. The agreement between theory and computation is very good. We also consider channels with the same scales as in Devillard *et al.* (1988). Our results are close to theirs for the band of wavenumbers where the localization phenomenon is the strongest, which is also where their results approximate well the wave tank experiments by Belzons *et al.* (1988).

The paper is organized as follows. The formulation and background of the scattering problem, together with the theoretical results, are reviewed in §2. In §3 a numerical Schwarz–Christoffel mapping is presented and we show how to use it in order to compute the relevant parameters defined by the stochastic theory (for example the localization length). Section 4 presents results comparing theory and computations. The expected value for the reflection coefficient, given in the theory, matches very well that obtained by a Monte Carlo simulation for wave propagation, using the boundary-element method. We close this section by comparing our results with those obtained by Devillard *et al.* (1988). Finally §5 contains the concluding remarks.

2. Formulation and background of the scattering problem

Consider gravity-driven surface waves, propagating in a shallow channel, in a regime where potential theory is applicable. The velocity potential $\phi(x, y, t)$ satisfies the linear equations (Whitham 1974):

$$\phi_{xx} + \phi_{yy} = 0 \quad \text{for} \quad -h_0 H(x/l_b) < y < 0,$$

with the free surface condition

$$\phi_{tt} = -g\phi_y \quad \text{at} \quad y = 0,$$

the Neumann condition at the bottom

$$\phi_y + \frac{h_0}{l_b} H'(x/l_b)\phi_x = 0 \quad \text{along} \quad y = -h_0 H(x/l_b)$$

and the following initial conditions given at the free surface:

$$\phi(x,0,0) = A\, f\left(\frac{x+c_0 t}{l_p}\right)\Big|_{t=0} \quad \text{and} \quad \phi_t(x,0,0) = \frac{Ac_0}{l_p} f'\left(\frac{x+c_0 t}{l_p}\right)\Big|_{t=0}.$$

The function f is smooth and has compact support in $[0,\infty)$. The constant A has dimensions of length squared over time so that f is dimensionless. The bottom topography is described by $y = -h_0 H(x/l_b)$, where

$$H(x/l_b) = \begin{cases} 1 + n(x/l_b) & \text{when} \quad -L < x < 0 \\ 1 & \text{when} \quad x \leqslant -L \quad \text{or} \quad x \geqslant 0. \end{cases}$$

We have introduced the length scales l_p (pulse width), h_0 (depth), l_b (horizontal length scale for bottom irregularities) and L (total length of the rough region). The acceleration due to gravity is denoted by g and the reference shallow water speed is $c_0 = (gh_0)^{1/2}$. The bottom profile is a rapidly varying zero-mean random process $n(x/l_b)$ about the undisturbed depth $y = -h_0$ and such that $|n| < 1$. Note that the depth fluctuations $n(x/l_b)$ are not necessarily small.

The ratios of length scales identify the regime of interest in wave reflection when ordered by a small parameter $\varepsilon > 0$:

$h_0/l_b = O(1) = \gamma_h$ (bottom irregularities are comparable to the depth),

$l_p/l_b = \gamma_p/\varepsilon$ (incident pulse is broad compared to the bottom irregularities),

$L/l_b = \gamma_L/\varepsilon^2$ (pulse penetrates in a long, rough channel).

The parameters γ_h, γ_p and γ_L are of order one and are related to the microscopic, intermediate and macroscopic scales respectively.

In order to formulate the reflection-transmission problem it is convenient to use dimensionless variables and to conformally map the rough channel onto a flat one. Details can be found in Nachbin & Papanicolaou (1992*b*). In the orthogonal curvilinear variables (ξ,ζ) the equations have the form

$$\phi_{\xi\xi} + \phi_{\zeta\zeta} = 0, \qquad -\gamma_h < \zeta < 0 \tag{2.1}$$

with the free surface condition

$$-(1+m(\xi))\,\phi_{tt} = \frac{1}{\gamma_h}\phi_\zeta \quad \text{at} \quad \zeta = 0, \tag{2.2}$$

the Neumann condition at the bottom

$$\phi_\zeta = 0 \quad \text{at} \quad \zeta = -\gamma_h, \tag{2.3}$$

and the initial conditions

$$\phi(\xi,0,0) = \frac{1}{(\varepsilon\gamma_p)^{1/2}}\, f\left(\varepsilon\,\frac{\xi+t}{\gamma_p}\right)\Big|_{t=0} \tag{2.4}$$

and

$$\phi_t(\xi,0,0) = \frac{(\varepsilon)^{1/2}}{(\gamma_p)^{3/2}} \; f'\left(\varepsilon \, \frac{\xi + t}{\gamma_p}\right)\Big|_{t=0} \tag{2.5}$$

given at the free surface. The new free surface coefficient $m(\xi) = 1 - \gamma_h y_\zeta(\xi,0)$ is related to the bottom irregularities through (Hamilton 1977; Nachbin & Papanicolaou 1992*b*)

$$m(\xi) \; = \; \frac{\pi}{4\gamma_h} \; \int_{-\infty}^{\infty} \frac{n(x(\xi_0,-\gamma_h))}{\cosh^2[(\pi/2\gamma_h)(\xi_0 - \xi)]} \mathrm{d}\xi_0. \tag{2.6}$$

In the limit as ε goes to zero, the coefficient $m(\xi)$ is varying on an extremely fine scale, when compared to the rough channel's macroscopic length scale. Therefore, this coefficient is considered to be a stochastic process. A system of stochastic differential equations is derived for the amplitudes of the propagating and evanescent modes, obtained from the eigenfunction decomposition of the time-harmonic velocity potential (Nachbin & Papanicolaou 1992*b*). The solution to these equations are characterized asymptotically as diffusion processes, through the application of a limit theorem for stochastic differential equations. Details of the stochastic theory can be found in Asch *et al.* (1991), Kohler(1977) and references therein.

The stochastic theory, given in the references above, is valid when the rapidly varying random coefficient has mean zero. For topographies of moderate amplitude, as in the examples presented in Nachbin & Papanicolaou (1992*b*), the coefficient $m(\xi)$ is effectively a mean-zero function. In the large-amplitude situation this is not true. This is better seen with periodic topographies. An example will be presented in § 4. To emphasize this aspect of the theory, we rewrite the free surface coefficient as

$$m(\xi) = \langle m \rangle + m_0(\xi). \tag{2.7}$$

We define the average as

$$\langle m \rangle = \frac{1}{\gamma_L} \int_{-\gamma_L}^{0} m(\xi)\mathrm{d}\xi \tag{2.8}$$

and $m_0(\xi)$ as the mean-zero part. We assume that the channel is long enough so that $\langle m \rangle$ is independent of the realization of the topography considered. This is based on the fact that the stochastic process is assumed to be ergodic.

The free surface condition is written as

$$-\left(1 + \frac{1}{1 + \langle m \rangle} \; m_0(\xi)\right) \; \phi_{tt} \; = \frac{1}{\gamma_h} \; \phi_\zeta \quad \text{at} \quad \zeta = 0, \tag{2.9}$$

where time has been rescaled by $t' = t/(1 + \langle m \rangle)^{1/2}$ and we have dropped the prime.

Summary of theoretical results

This section contains a brief summary of the results obtained in Nachbin & Papanicolaou (1992*b*). The expected value of the transmission coefficient, for an incident monochromatic wavetrain of frequency ω, is obtained through the application of an asymptotic theory for the solution of stochastic differential equations. We repeat our results for convenience:

$$E\{|T|^2\} \; = \; \exp\left(-\frac{\gamma_L \; \omega^2}{8\gamma_h^2}\alpha_{mm}\right) \; \int_{-\infty}^{\infty} \exp\left(-t^2 \frac{\gamma_L \; \omega^2}{2\gamma_h^2}\alpha_{mm}\right) \frac{\pi t \; \sinh \pi t}{\cosh^2 \pi t} \; \mathrm{d}t.$$

The formula above can be used to estimate how much transmission is obtained at the end of the rough region of the channel, once the effective parameter for scattering

$$\alpha_{mm} = \frac{1}{(1+\langle m\rangle)^2}\int_0^\infty E\{m_0(s)m_0(0)\}\mathrm{d}s \tag{2.10}$$

is known. The phenomenon of localization is characterized through the exponential decay of the transmission coefficient as a function of the rough region's total length γ_L. Using Laplace's method, the expected value of the transmission coefficient can be approximated for large values of γ_L/ℓ:

$$E\{|T|^2\} \sim \frac{\pi^{5/2}}{2(\gamma_L/\ell)^{3/2}}\exp(-\gamma_L/(4\ell)), \tag{2.11}$$

where the localization length ℓ is given by

$$\ell = \frac{2\gamma_h^2}{\alpha_{mm}\omega^2}. \tag{2.12}$$

The localization length ℓ gives an idea of the wave's penetration depth into the random medium. For a given frequency ω we can see how geometrical features of the channel affect the localization length through the parameters α_{mm} and γ_h. The expression (2.11) is exactly the same as the one obtained for the linear Schrödinger equation with a random potential (cf. Gredeskul & Kivshar 1992). It also appears in Papanicolaou & Keller (1971) when waves propagate through a layer with random index of refraction. Devillard *et al.* (1988) analysed water waves in channels with random piecewise-constant topography and estimated the localization length numerically.

For the propagation of a pulse we give the expected value for the reflection process (where $E\{R^2(t)\} = 1 - E\{T^2(t)\}$):

$$E\{R^2(t)\} = \frac{1}{2\pi}\int_{-\infty}^{\infty}|\hat{f}(\omega)|^2\,\frac{\gamma_h\omega^2\alpha_{mm}}{\left[\gamma_h+\omega^2\alpha_{mm}\,t\right]^2}\,\mathrm{d}\omega. \tag{2.13}$$

We point out that in the results above, only the correlation function of the random $O(1)$ depth perturbation plays a role in the final result, through the effective parameter for scattering α_{mm}. Note that the initial pulse shape f is known (cf. (2.4)) with its Fourier transform given by

$$\hat{f}(\omega) = \int_{-\infty}^{\infty} e^{i\omega\tau}f(\tau)\mathrm{d}\tau.$$

We can readily calculate the decay in time of the expected value of the reflection process, by numerical integration of the expression above.

In Nachbin & Papanicolaou (1992*b*) we used the boundary-element method in the numerical study of reflection and transmission of long waves in shallow channels with irregular bottom topographies. For each realization of the bottom topography we allowed a Gaussian pulse (for the potential) to propagate over the rough region and we recorded the reflected signal, at a point x_j close to the beginning of the rough region. We then computed the statistical properties of the numerical reflected signals. We graphed time-dependent curves for $E\{R^2(t)\}$ and we compared them with the statistical properties of our numerical experiments. Namely we verify if

$$E\{R^2(t)\} \approx \frac{1}{M}\sum_{m=1}^{M}\phi^2(x_j,0,t;\omega_m), \tag{2.14}$$

when the number of realizations M is large enough. Each realization of the channel's topography is labelled by ω_m. We found good agreement between the theory and numerical computations for channels with moderate depth variations.

As mentioned earlier, the theory given in Nachbin & Papanicolaou (1992*b*) is valid for large-amplitude bottom variations. Nevertheless it is extremely difficult to calculate analytically the effective parameter for scattering α_{mm} in the large-amplitude case. In the following section we present an algorithm showing how to calculate the effective parameter for scattering, for any bottom configuration.

3. Numerical method for finding effective parameters

3.1. *The numerical evaluation of the variable free surface coefficient* $m(\xi)$

In this section an arbitrary symmetric channel, bounded by straight wall segments in the physical z-plane ($z(\xi,\zeta) = x(\xi,\zeta) + \mathrm{i}y(\xi,\zeta)$), is mapped onto a straight channel in the computational w-plane ($w = \xi + \mathrm{i}\zeta$). For the purpose of finding the Schwarz–Christoffel transformation (Ahlfors 1979; Henrici 1986) it is convenient to take the origin of the z-plane to be at the the first left-corner of the bottom topography, where it changes from flat to rough. The dimensionless water wave flow domain is such that the free surface is given by $y = 1$. For the geometry described we consider a transformation $z(w)$, of the Schwarz–Christoffel type (Floryan 1985; Sridhar & Davies 1985), such that its derivative is given by

$$\frac{\mathrm{d}z}{\mathrm{d}w}(\xi,\zeta) \;=\; \frac{h_0}{\gamma_h}\prod_{l=1}^{N}\left[\sinh\frac{\pi}{2\gamma_h}(w-a_l)\right]^{\alpha_l}. \tag{3.1}$$

The flat channel in the non-physical w-plane has width γ_h. The N unknown parameters a_l are the pre-images of the bottom topography's corners. Furthermore, the $\pi\alpha_l$ represent the turning angles at each corner (with pre-image a_l). Their values are known and we use the convention that they are positive for the clockwise rotation when the boundary of the channel is traversed in the counterclockwise direction.

By the Riemann mapping theorem (Ahlfors 1979) we know that the conformal mapping $z(w)$ is uniquely defined once we choose the value of the scaling constant C (for simplicity we take $C = h_0/\gamma_h = 1$) and once we impose that the origins of the two planes coincide (namely $z(0,0) = 0$).

From complex analysis we have that

$$\frac{\mathrm{d}z}{\mathrm{d}w} = \frac{\partial y}{\partial\zeta} \;-\mathrm{i}\,\frac{\partial x}{\partial\zeta}.$$

On the other hand, the change of variables for the water wave equations lead to the following variable coefficient in the free surface condition:

$$\frac{\partial y}{\partial\zeta}(\xi,1) \;=\; 1 \;+\; m(\xi).$$

By putting the expressions above together, straightforward algebra leads to a simple formula for the variable free surface coefficient $m(\xi)$:

$$m(\xi) \;=\; \left(\prod_{l=1}^{N}\left[\cosh\frac{\pi}{2}(\xi-a_l)\right]^{\alpha_l}\right) - 1. \tag{3.2}$$

The coefficient $m(\xi)$ can be easily evaluated, at any given point along the free surface,

once the pre-images a_l, $l = 1,\ldots,N$ are known. The free surface coefficient $m(\xi)$ is written in a way that avoids the numerical evaluation of fractional powers of complex numbers. Hence we do not have to worry about keeping track of branch points.

The N unknown parameters a_l are determined by a method of successive approximations. A simple iteration scheme is presented in Floryan (1985) and Sridhar & Davies (1985). The basic underlying strategy is to find values of the pre-images of the corners, so that the length of each straight wall segment satisfies

$$\frac{|a_l^{(v)} - a_{l-1}^{(v)}|}{|z_l - z_{l-1}|} = \frac{|a_l^{(v-1)} - a_{l-1}^{(v-1)}|}{|z_l^{(v-1)} - z_{l-1}^{(v-1)}|}.$$

Superscripts indicate the vth iterated value for each corner's pre-image and its corresponding location $z_l^{(v)}$ in the physical plane. The values $z_l^{(v)}$ are obtained by a specially devised numerical quadrature, that allows the integration of (3.1) across the singularities located at corners with negative values of α_l. Details are given in Floryan (1985) and Sridhar & Davies (1985).

The iteration scheme takes into account the fact that the origins of the two planes coincide. This implies that $z_1 = a_1 = 0$ at all stages of the iterative scheme. All the other corners are to the right of z_1 and their pre-images are obtained successively by using

$$a_l^{(v)} = a_{l-1}^{(v)} + \frac{|a_l^{(v-1)} - a_{l-1}^{(v-1)}||z_l - z_{l-1}|}{|z_l^{(v-1)} - z_{l-1}^{(v-1)}|}. \tag{3.3}$$

Left-right sweeps for the values of the pre-images are done successively, using (3.3), until convergence is achieved. When there are no discontinuities along the bottom topography, we take as the initial guess for each parameter a_l the value $a_l^{(0)} = x_l$. For topographies with discontinuities, we take $a_l^{(0)}$ to be the length of the wall segment ending at z_l.

We should point out that the method given in Floryan (1985) can be extended (cf. his §3) to channels with curved wall segments. Nevertheless we restricted our numerical experiments to cases where the channel had straight wall segments, since that is the optimal configuration for the boundary-element method to vectorize on a supercomputer (cf. Nachbin 1993; Nachbin & Papanicolaou 1992*a*, §2).

Regarding the convergence of the Schwarz–Christoffel code, it can take up to 30 iterations depending on the size of the topography's amplitude. One way of improving the performance of the numerical conformal mapping technique is by using the fast method proposed in O'Donnel & Rokhlin (1989).

3.2. *The numerical evaluation of the correlation function $E\{m(s)m(0)\}$ and of the localization length ℓ*

The correlation function of the free surface coefficient is obtained by a Monte Carlo simulation. Samples of random bottom topographies are created using a random number generator. Each realization of the topography (labelled by ω_m) is conformally mapped through the numerical Schwarz–Christoffel transformation. Using (3.2) and a set of P equally spaced points along the mapped free surface (with spacing $\Delta\xi$) we have

$$m_0(\xi_j;\omega_m) = \left(\prod_{l=1}^{N}\left[\cosh\frac{\pi}{2}(\xi_j - a_l)\right]^{\alpha_l}\right) - 1 - \langle m\rangle, \quad j = 1,\ldots,P. \tag{3.4}$$

The average $\langle m \rangle$ is computed using the trapezoidal rule. The correlation function is evaluated, over the equally spaced points, as follows:

$$E_{MC}\{m_0(j\Delta\xi)m_0(0)\} \approx \frac{1}{MP_{ab}} \sum_{m=1}^{M} \sum_{p=p_a}^{p_b-j} m_0(\xi_{p+j};\omega_m)m_0(\xi_p;\omega_m). \tag{3.5}$$

The notation is such that E_{MC} is the expected value computed through a Monte Carlo simulation using M realizations, p_a indicates the number of the first point and p_b of the last point of $m(\xi)$ considered in calculating the correlation function. P_{ab} is the total number of points utilized ($P_{ab} = p_b - p_a + 1 - j$). It is convenient to take p_a and p_b so that ξ_p and ξ_{p+j} are away from the ends of the rough region. Note that (2.6) shows how the (deterministic) flat region can affect non-zero values of $m(\xi)$ depending on the effective width of the kernel.

The effective parameter for scattering is obtained by integrating the correlation function using the trapezoidal rule. The correlation function is monotonically decreasing, so we complete the improper integration as soon as the integrand is approximately zero. For best results, we use several different points p_a and p_b. As these points are moved away from the ends, α_{mm} grows and then oscillates about a certain value, which we take to be its final value. Finally, the localization length is found by using (2.12).

4. Results for large-amplitude depth variations and comparison with the theory

4.1. *Periodic bottom topographies*

The numerical conformal mapping of periodic channels is carried out. The examples given below improve our insight into the effect of having channels with small but finite depth. As opposed to the infinitesimal case (i.e. long-wave theory), the topography is felt along the free surface as a smooth obstruction. This can be seen from expression (2.6) and in the figures below, generated by the numerical conformal mapping technique.

Consider a rough periodic segment of length 30 units, having triangles of base equal to 2 length units and height 0.6 units. Note that the depth variations are of large amplitude. Figure 1 superimposes the original bottom's polygonal profile $n(x)$ and the variable free surface coefficient $m(\xi)$. The horizontal x- and ξ-coordinates are on different scales since the channel is 'stretched' during the Schwarz–Christoffel mapping. We can clearly see the (smoothing) depth-effect predicted by (2.6).

In Nachbin & Papanicolaou (1992a) no reflection is observed when long waves propagate over rapidly varying periodic topographies. This result is not surprising. The reflection-transmission problem can be formulated as a system of ordinary differential equations (a matrix Riccati equation; cf. Nachbin & Papanicolaou 1992*b*) with periodic coefficients, and the method of averaging can be used to show that, in the limit as the bottom's period goes to zero, no reflection is observed.

However, the conformal mapping technique shows that an additional ingredient plays a role in the averaging process: the channel's depth. There is a horizontal and a vertical length scale playing a role in what we will call the homogenization (i.e. averaging) of the periodic bottom. The term homogenization is borrowed from the field of composite materials, where waves propagating in materials with rapidly varying inhomogeneities behave as if they were travelling in a homogeneous material having an effective conductivity different from that of the pure material. Therefore

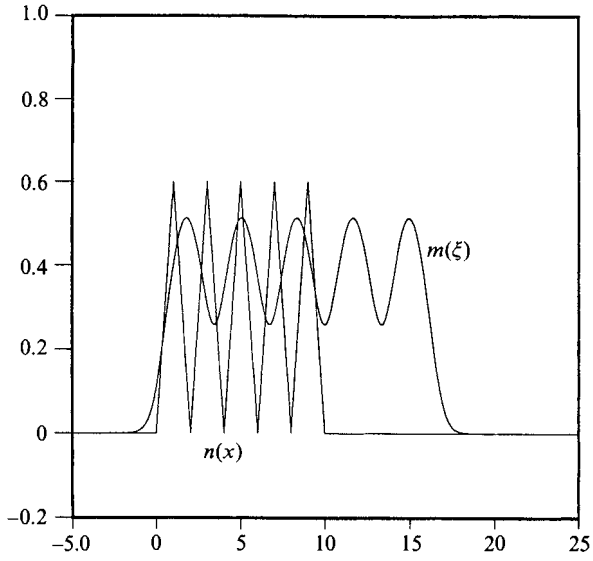

FIGURE 1. Comparison between the polygonal topography profile $n(x)$ and the variable free surface coefficient $m(\xi)$.

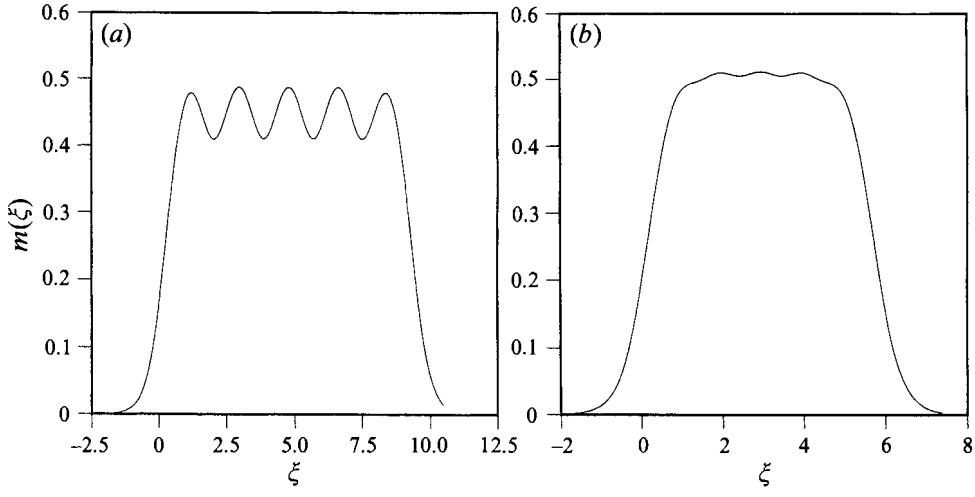

FIGURE 2. The homogenization effect for the variable free surface coefficient $m(\xi)$. The bottom irregularities are on the length scale (*a*) $l_b = 1.0$ and (*b*) $l_b = 0.5$.

in such a regime, the long water wave will feel the periodic region as an effectively flat one. To be more precise, there will be a quick transition from the originally flat region where $m(\xi) \equiv 0$, to the effectively flat region where $m(\xi) \approx$ non-zero constant. These two flat regions are analogous to two homogeneous materials having different conductivities (Nachbin & Papanicolaou 1992a). The effect of the vertical and horizontal length scales can be visualized in figure 2. The periodic topography now has triangles with bases of 1.0 and 0.5 length units respectively. The bottom is felt at free surface level through the coefficient $m(\xi)$. The homogenization effect is evident. Very quickly the corrugations of $m(\xi)$ decrease in amplitude and when seen from the free surface the topography becomes effectively a smooth step. Hence, as

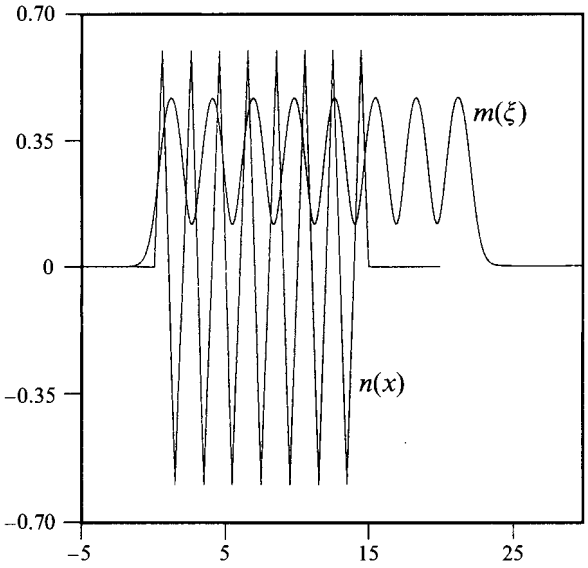

FIGURE 3. A mean-zero polygonal topography $n(x)$ gives rise to a non-mean-zero free surface coefficient $m(\xi)$.

expected, when a long wave propagates over the rapidly varying region no reflection is observed. Nevertheless, it will propagate with an effective shallow water speed (in analogy with effective conductivity) smaller than the standard shallow water speed, as predicted by Rosales & Papanicolaou (1983), and observed numerically by Nachbin & Papanicolaou (1992*a*).

The final experiment with periodic bottoms considers a mean-zero topography. It is well known that the effect of disturbances along the border of a domain, where we are solving for a harmonic function, decays exponentially fast towards the interior. For example, in a channel with a flat bottom the harmonic extension of disturbances like $\cos(x-t)$ (along the free surface $y=0$) is obtained by multiplying it by $\cosh(h_0+y)$. An analogous situation takes place in the conformal mapping problem which also deals with harmonic functions (cf. the problem given by (11), (12) in Nachbin & Papanicolaou 1992*b*). In this purely geometrical problem the presence of the valleys of the topography are felt, along the free surface, in a (exponentially) weaker form than the summits. A manifestation of this fact is that the free surface coefficient $m(\xi)$ is not mean-zero even though the botton profile $n(x)$ is. Therefore, the topography is seen from the free surface as a step superimposed with small periodic corrugations (cf. figure 3).

We summarize the discussion above by relating it more closely to the (physical) context of water waves. First we should note that two problems are being considered. A dynamical problem of surface waves interacting with a bottom topography and a geometrical problem (i.e. the conformal mapping) from which we gain insight into how the bottom topography is seen from the free surface $y=0$, through the coefficient $m(\xi)$. As mentioned above, no effective reflection is observed for the (dynamical) problem of a long wave propagating over a rapidly varying periodic topography (Nachbin & Papanicolaou 1992*a*). This is expected since the wave cannot feel the inhomogeneities of the medium (i.e. the depth variations) in detail. We pointed out that the conformal mapping shows how the length scale associated with the depth also

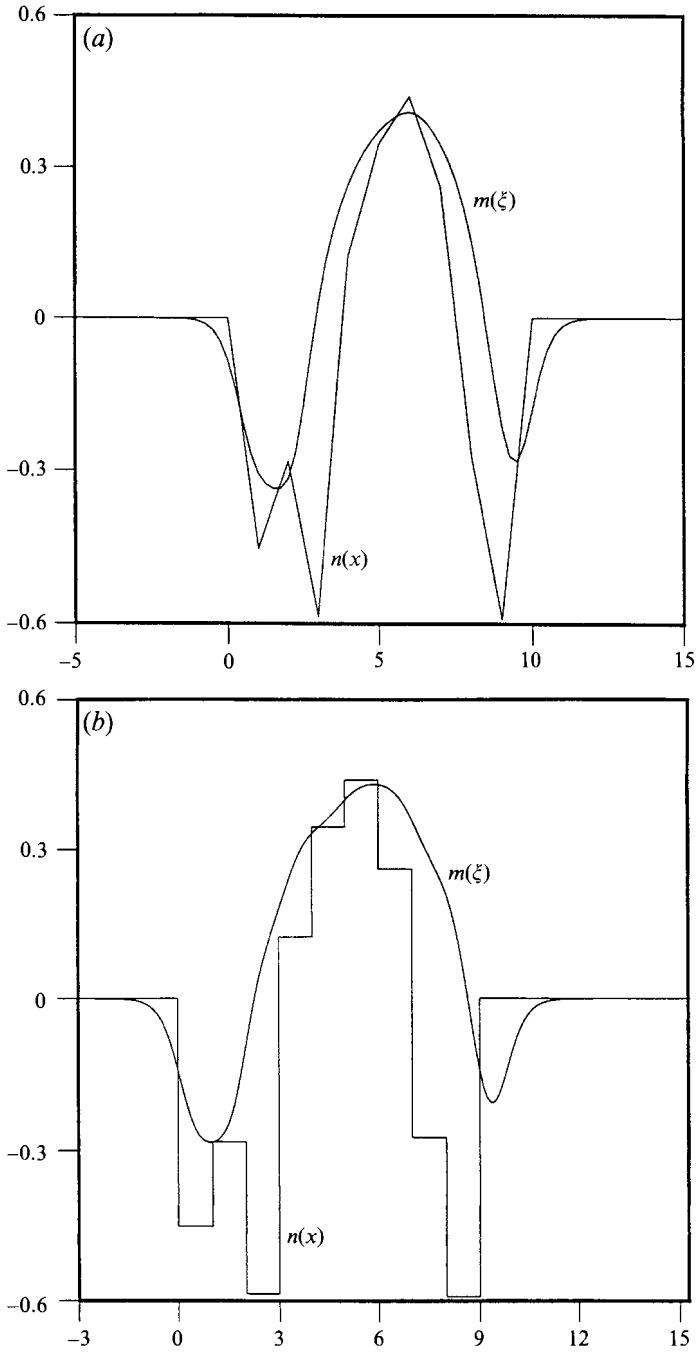

FIGURE 4. Comparison between $n(x)$ and $m(\xi)$ for a (*a*) piecewise-linear random topography and (*b*) piecewise-constant random topography.

participates in this averaging phenomenon. All the results of the conformal mapping (cf. figures 1, 3 and 4) show that the free surface coefficient has little sensitivity to details, and in particular to the valleys, of the submerged topography. A possible physical interpretation of this fact is that we have an added-mass-type phenomenon

in the deeper regions of the valleys. These regions are not felt in detail from the free surface, and for the reflection-transmission problem can be considered as part of the submerged obstacles.

We will show in the next subsection that the geometrical smoothing features discussed above are also true for random topographies. We started with the periodic case because it is easier to visualize. Nevertheless there is a crucial difference between rapidly varying periodic and random topographies, when we look at the dynamical problem of wave propagation. The averaging argument does not work for random topographies. The disordered nature of the scattering phenomenon will have a cummulative effect, when the random medium is long enough. The residual effect of disordered scattering is precisely the phenomenon of localization.

4.2. *Random bottom topographies*

For the numerical experiments we consider both random piecewise-linear and random piecewise-constant topography profiles. The latter are of the same type as the profiles used in the laboratory experiments by Belzons *et al.* (1988) and the theory by Devillard *et al.* (1988). In figure 4, $n(x)$ and $m(\xi)$ are graphed together, for two short (prototype) channels, so that the smoothing and added-mass effects, discussed in §4.1 above, can be visualized.

This section contains results of two sets of Monte Carlo simulations of different nature. One set of simulations is done to compute a purely geometrical quantity, namely the correlation function for the free surface coefficient $m(\xi)$. The main objective is to compute the effective parameter for scattering α_{mm} and the localization length ℓ defined in the theory. The Monte Carlo method makes use of the numerical Schwarz–Christoffel mapping described in §3.

The second set of Monte Carlo simulations is a dynamical one. It makes use of the boundary-element method to generate reflected waves. We compute statistical properties of these waves and compare with theoretical results. Details are given in Nachbin & Papanicolaou (1992*a*,*b*).

At this point we should pause to note that three problems come together, each having a scaling adequate for the analysis performed. The first one is the analytical study having the microscopic, intermediate and macroscopic scales as given in § 2. The second is the conformal mapping problem which, for convenience, maps a flat strip of unit width onto a corrugated one also of unit width. Finally we have the numerical problem which is formulated in the (standard) dimensionless variables (Nachbin & Papanicolaou 1992*a*; Whitham 1974) which lead to the definition of the dispersion parameter $\beta = h_0/\lambda$. The typical wavelength is given by λ. This is the most convenient set-up for the boundary-element method, in order for it to capture several features of wave propagation in rough channels. A numerical dispersion study is given in Nachbin & Papanicolaou (1992*a*) and a series of experiments are presented in Nachbin & Papanicolaou (1992*a*,*b*).

In order to make the procedure of matching the theoretical results with computations as simple (and systematic) as possible, we present a summary of the different scalings considered. In the asymptotic theory the result is given with respect to a reference pulse of unit width. As mentioned above, we always take the Schwarz–Christoffel mapping to be such that the flat channel is of unit depth. Therefore we must find the corresponding length scale $\tilde{l}_b$ for the depth variations. The following set of correspondences are useful:

(*a*) In the stochastic theory the problem is scaled so that the pulse width is one.

We call the corresponding depth $h^\star$ and topography length scale $l_b^\star$, where

$$\frac{h_0}{\lambda} = \beta = \frac{h^\star}{\lambda^\star = 1}$$

and

$$l_b^\star = l_b/l_p.$$

(*b*) For the Schwarz–Christoffel problem we have

$$h^\star \longmapsto 1, \quad l_b^\star \longmapsto \tilde{l}_b.$$

Using the relations above and making the correspondence between the scales used in the conformal mapping, analytical and computational parts of this work, it turns out that the corresponding bottom's characteristic length, in the conformal mapping problem, should be

$$\tilde{l}_b = l_b/(l_p\beta).$$

Let the physical problem of interest be such that the topography variations are on the length scale l_b, the wave pulse is of width l_p and with dispersion coefficient β. The typical channel to be mapped by the Schwarz–Christoffel code has a rough topography of average depth equal to one, varying on a horizontal length scale equal to $\tilde{l}_b$.

Once the Monte Carlo simulation for $E\{m_0(s)m_0(0)\}$ has converged to an acceptable value, the result has to be rescaled back so that the theoretical and numerical expressions for $E\{R^2(t)\}$ are in the same scale:

$$\alpha_{mm} = \frac{1}{(1+\langle m\rangle)^2}\int_0^\infty h^\star\, E_{MC}\{m_0(s)m_0(0)\}\mathrm{d}s, \quad h^\star = \beta \tag{4.1}$$

where E_{MC} denotes the expected value obtained by the Monte Carlo method. The trapezoidal rule is used for the integration, which needs only a few points since the correlation function decays to zero very fast.

The observation concerning the rapid decay of E_{MC} is very important in terms of numerical efficiency. Short channels can be used in the Schwarz–Christoffel, Monte Carlo simulations without any loss of generality. Figure 5 shows the coefficient $m(\xi)$ for two channels, one being twice as long as the other but having exactly the same profile over its first half. Both coefficients $m(\xi)$ agree very well almost up to the end of the shorter channel. Although in the boundary-element method we use very long channels, the parameter α_{mm} can be computed using much shorter ones.

We proceed to present results comparing theory and computations. The numerical experiments were designed to provide evidence of the wide range of applicability (regarding general bottom configurations) of the theory developed in Nachbin & Papanicolaou (1992*b*). Different classes of bottom profiles with large-amplitude perturbations are considered. Several parameters are allowed to vary, including the dispersion parameter β.

We start with Monte Carlo simulations for piecewise-linear profiles of large amplitude ($\delta = 0.6$). The geometry is such that $l_b = h_0 = 0.1$, $l_p = 1.0$, the rough segment of the channel is 20 units long, $\beta = 0.08$ and the numerical solution is computed over an interval of 45 time units. The Schwarz–Christoffel code gives $\alpha_{mm} = 0.0066$, where $\tilde{l}_b = 1.25$ and $h^\star = \beta$. The localization length is $\ell = 303.03/\omega^2$. In figure 6(*a*) we can see the agreement between theory (60 realizations) and computations (60 realizations).

To reinforce our statement that the theoretical results apply to general topographies, we consider piecewise-constant profiles ($\delta = 0.5$). The parameters used were $l_b = h_0 =$

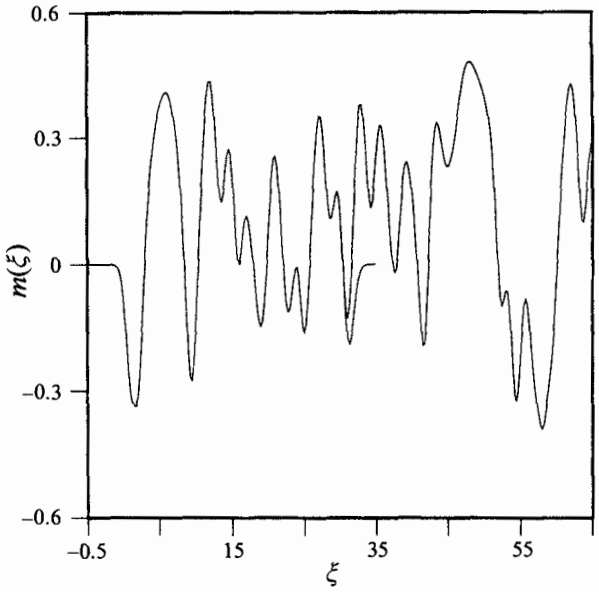

FIGURE 5. Comparison between the free surface coefficients $m(\xi)$ of two channels, where one is twice as long as the other but with identical topographies where they overlap.

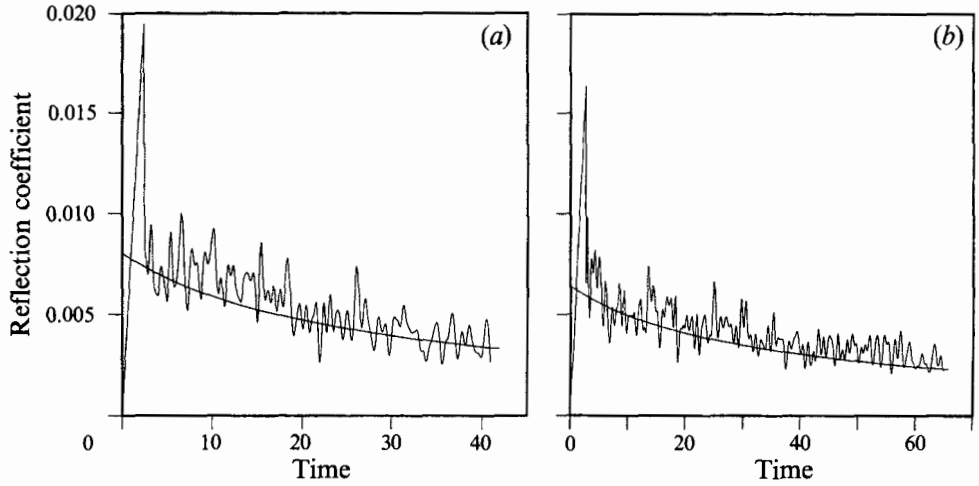

FIGURE 6. Comparison between theory (60 realizations) and computations (60 realizations) for (*a*) piecewise-linear topographies of amplitude $\delta = 0.6$; (*b*) piecewise-constant topographies of amplitude $\delta = 0.5$.

0.1, $l_p = 1.0$, the rough segment is 30 units long, $\beta = 0.1$ and the numerical solution is computed over an interval of 65 time units. Using $\tilde{l}_b = 1.0$ and $h^* = 0.1$ the numerical conformal mapping code gave $\alpha_{mm} = 0.0051$. The localization length is $\ell = 392.16/\omega^2$. In figure 6(*b*) we present the agreement between theory (45 realizations) and computations (60 realizations). A few profiles sampled failed to converge for the Schwarz–Christoffel method. We believe that this was due to the well-known 'crowding problem' in conformal mapping (cf. Howell & Trefethen 1990). We discarded these problematic samples (about 10% of the total) and generated some additional ones.

An interesting experiment is to compare the localization lengths for piecewise-constant and piecewise-linear topographies having the same characteristics, that is, $\delta = 0.5$, $l_b = h_0 = 0.1$, $l_p = 1.0$, the rough segment is 30 units long and $\beta = 0.1$. We recall that for piecewise-constant profiles the numerical conformal mapping code gave $\alpha_{mm} = 0.0051$ and the localization length is $\ell = 392.16/\omega^2$. Now for piecewise-linear profiles the numerical conformal mapping code gives $\alpha_{mm} = 0.0039$ and the localization length is $\ell = 512.82/\omega^2$. Therefore the localization length for piecewise-linear profiles is 30% larger than for piecewise-constant ones. This is expected since submerged obstacles with vertical walls generate more reflection than if they had inclined walls. Note that over each subinterval of length l_b we have a submerged obstacle: a triangular protuberance (or depression) in the piecewise-linear case or a rectangular protuberance (or depression) in the piecewise-constant case. Note also that § 10.3 of Nachbin & Papanicolaou (1992*b*) has a calculation (for the small-amplitude case) showing that if we increase the slope of the bottom then the parameter α_{mm} also increases. Therefore, there is less transmission in the piecewise-constant case, which is analogous to having a smaller localization length. Dividing the localization length by the length scale of the obstacles (i.e. l_b) gives an idea of how many obstacles of random height will effectively participate in the multiple scattering of water waves before their amplitudes are negligible.

4.3. *Comparison with related work*

We close this section by comparing our theory with related work (Belzons *et al.* 1988 and Devillard *et al.* 1988; Hasselmann 1966 and Long 1973). We start by briefly describing their results.

In their theoretical study, Devillard *et al.* (1988) considered both shallow water theory and potential theory, together with a transfer matrix technique, to estimate the localization length for water waves propagating over piecewise-constant topographies. The topography is such that the wide-spacing approximation is valid, that is the mean length of the steps is much greater than the height of the water. In the long-wave regime shallow water theory and potential theory agree, and the localization length behaves like $\ell \sim 1/\omega^2$, for $\omega \to 0$ (cf. Devillard *et al.* 1988, pp. 525, 532). In the short-wave regime, the potential theory analysis (shallow water theory is not valid) gives that the localization length diverges exponentially (cf. Devillard *et al.* 1988, p. 532 and Appendix) which means that the interaction with the topography is extremely weak. Their time-harmonic theory is not restricted to any wavelength and the localization length is computed numerically as 'the inverse of the Lyapunov exponent associated with the products of the renormalized transfer matrices'.

As mentioned in the introduction, Hasselmann (1966) used the formalism of quantum field theory to describe the scattering of internal and surface waves by topographic irregularities in a stratified fluid. The theory provides the time rate of change of a wave spectrum as a linear functional of the spectrum of the bottom irregularities with coupling coefficients determined by the eigenfunctions of the linear flat bottom problem. In deriving this functional, heuristic interaction rules are assumed and Hasselmann (1966) formulates a statistical energy transfer process. The expressions for the transfer processes can be interpreted in terms of collision processes and therefore resemble Boltzmann integrals for interacting particles (cf. Hasselmann 1966, §3). Both wave amplitudes and bottom displacements are considered small so that perturbation techniques are applicable. Long (1973) calculated the coupling coefficients, given by Hasselmann (1966), for the homogeneous fluid case of surface waves alone and concluded that the presence of a random topography could be

sufficient to account for swell decay (see also Mysak 1978). The swell decay in time is characterized by the solution of a transport equation, which gives the evolution of the wave spectrum (cf. Long 1973, (7)). Their theory for swell decay does not furnish any length scale that could be used to compare with the localization length obtained by other authors.

We will now show that our theory is consistent with the findings of Devillard *et al.* (1988). Recall that Belzons *et al.* (1988) validated their results in a series of wave tank experiments. They considered monochromatic waves propagating over piecewise-constant topographies, with no restriction on the wavelength.

Our main goal is to study pulse-shaped waves propagating over arbitrary rapidly varying topographies. The pulse width is such that the bulk of its spectrum is in the long-wave regime. Moreover, the high end of the spectrum has a very weak interaction with the bottom topography, as expressed by the exponential divergence of the localization length given in Devillard *et al.* (1988). These modes also have exponentially small amplitudes. We have concentrated our analysis on long waves and scaled accordingly. This is a mild restriction and our theory leads to a quadratic dependence of the localization length in terms of the frequency, as in Devillard *et al.* (1988). We are able to calculate the corresponding constant: $\ell = C/\omega^2$, where the constant C is $2\gamma_h^2/\alpha_{mm}$. Note that we can take into account different kinds of topography profiles (piecewise-constant, piecewise-linear, etc ...) through the parameter α_{mm}.

Additional evidence that our results are consistent with previous work is given in the following experiments, which use the same length scales as in (Devillard *et al.* 1988, figure 5). We consider piecewise-constant profiles of large amplitude ($\delta = 5/7 \approx 0.71$) having a correlation length of $l_b = 16/7 \approx 2.29$. We performed three different Monte Carlo experiments with our Schwarz–Christoffel code. In the first set we keep the horizontal length scale of the random steps fixed (at 2.29), and we take 60 realizations having 30 steps, each. Owing to the crowding problem only 1/3 of the realizations converge under the iterative conformal mapping scheme. This might lead to a biased result. Nevertheless we proceed with our calculation and get $\alpha_{mm} = 0.0672$ and $\ell = 0.753(\lambda/l_b)^2$. Hoping to obtain a better convergence rate we map a series of channels that are not so elongated. Our second set of Monte Carlo experiments uses 60 realizations of channels having 16 random steps each. We now obtain 50% of convergence, with $\alpha_{mm} = 0.0616$ and $\ell = 0.823(\lambda/l_b)^2$. Finally we allow the length of the steps (as well as the heights) to be random, as in Devillard *et al.* (1988). In other words we allow the length of the steps to be uniformly distributed in $[0.5l_b, 1.5l_b]$. Certain samples might violate the wide-spacing assumption, but this was the scale adopted by the authors above. The third set of Monte Carlo experiments uses 60 realizations of channels having 16 random steps each. Again we get 50% convergence with $\alpha = 0.0563$ and $\ell = 0.899(\lambda/l_b)^2$.

The agreement between the three sets of experiments and the results by Devillard *et al.* (1988) is good. In figure 7 we compare the curves

$$\ell = \frac{h_0^2}{2\pi^2\alpha_{mm}}(\lambda/l_b)^2,$$

given by the three experiments above, with five values obtained from figure 5 in Devillard *et al.* (1988). The wavelengths chosen are related to the band of frequencies where the results of the wave tank experiments of Belzons *et al.* (1988) (cf. figure 15 therein) are close to the theory of Devillard *et al.* (1988).

Finally we point out that the localization length is a length scale defined for

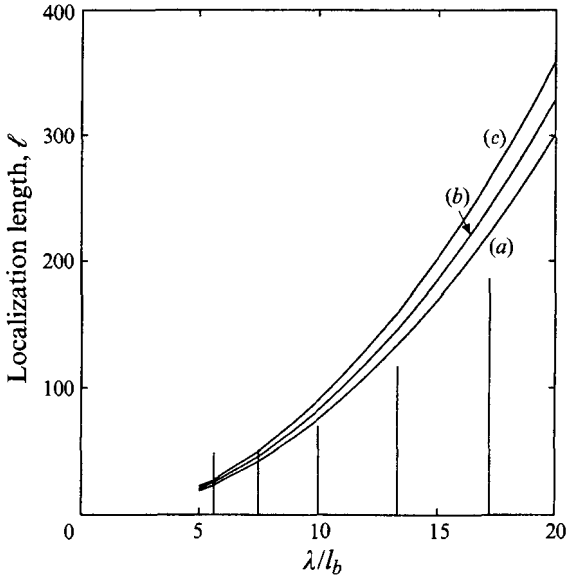

FIGURE 7. Comparison with the results of Devillard *et al.* (1988): (*a*) (experiment 1) $\ell = 0.753(\lambda/l_b)^2$); (*b*) (experiment 2) $\ell = 0.823(\lambda/l_b)^2$); (*c*) (experiment 3) $\ell = 0.899(\lambda/l_b)^2$). The vertical bars are obtained from figure 5 in Devillard *et al.* (1988).

time-harmonic (monochromatic) waves. Nevertheless the theory given in Nachbin & Papanicolaou (1992*b*) applies also to pulse-shaped waves. It predicts the expected value of the, now, time-dependent reflection coefficient. The rate at which it decays in time depends on the effective parameter for scattering α_{mm} (cf. (2.13)). Long (1973) studies the time decay in Fourier space, that is of the wave spectrum, while we look at the time decay of the reflection coefficient.

5. Concluding remarks

The theoretical results for the reflection-transmission problem of linear water waves in shallow channels obtained in Nachbin & Papanicolaou (1992*b*) can now be applied to their full extent, that is to consider large-amplitude bottom topographies with different types of random profiles. The use of a numerical Schwarz–Christoffel transformation enabled the evaluation of parameters defined in the asymptotic theory, for several bottom configurations. No restrictions such as mild-slope topographies are required, nor does the bottom have to be discretized into piecewise-constant segments.

The following results are given. First, the localization length for both piecewise-linear and piecewise-constant bottom profiles are calculated. In terms of applications, the localization length gives the rate of (exponential) decay of the waves' amplitude, as it propagates over long random topographies. Secondly, reflected waves are generated numerically, using the boundary-element method, and their statistics (i.e. $E\{R^2\}$) agree very well with theoretical results. Finally, our results are compared with the work of Devillard *et al.* (1988).

The conformal mapping technique also provides further insight into the multiple-scattering problem, when water wave propagation is modelled using potential theory. This method permits the visualization of depth effects through the mapping of a polygonal bottom topography onto a smooth variable free surface coefficient. As the bottom

varies on a shorter scale the homogenization effect becomes evident. For example, a rapidly varying periodic bottom is viewed, from the free surface, as a smooth step.

I would like to thank G. Papanicolaou for useful discussions on this topic. Part of this work was done while the author was a Research Instructor at Ohio State University. I would also like to thank G. Baker for his support and helpful comments, and the Ohio Supercomputer Center for providing supercomputing hours on their Cray Y-MP through grant # PAS599-3. This work was supported, in part, by the New Jersey Institute of Technology under Grant No. 421560. I would also like to thank the referees for useful comments in improving this paper and for pointing out references that I was not aware of.

REFERENCES

AHLFORS, L. V. 1979 *Complex Analysis*, 3rd Edn. McGraw Hill.

ASCH, M., KOHLER, W., PAPANICOLAOU, G., POSTEL, M. & WHITE, B. 1991 Frequency content of randomly scattered signals *SIAM Rev.* **33**, 519–625.

BELZONS, M., GUAZZELLI, E. & PARODI, O. 1988 Gravity waves on a rough bottom: experimental evidence of one-dimensional localization, *J. Fluid Mech.* **186**, 539–558.

DALRYMPLE, R. A. & KIRBY, J. T. 1986 Water waves over ripples. *J. Waterway Port Coastal Ocean Engng* **112**, 309–319.

DEVILLARD, P., DUNLOP, F. & SOUILLARD, B. 1988 Localization of gravity waves on a channel with a random bottom. *J. Fluid Mech.* **186**, 521–538.

FLORYAN, J. M. 1985 Conformal-mapping based coordinate generation method for channel flows. *J. Comput. Phys.* **58**, 229–245.

GREDESKUL, S. A. & KIVSHAR, Y. S. 1992 Propagation and scattering of nonlinear waves in disordered systems. *Phys. Rep.* **216**, 1–61.

GUAZZELLI, E., REY, V. & BELZONS, M. 1992 Higher-order Bragg reflection of gravity surface waves by periodic beds. *J. Fluid Mech.* **245**, 301–317.

HAMILTON, J. 1977 Differential equations for long-period gravity waves on a fluid of rapidly varying depth. *J. Fluid Mech.* **83**, 289–310.

HASSELMANN, K. 1966 Feynman diagrams and interaction rules of wave-wave scattering processes. *Rev. Geophys. Space Phys.* **4**, 1–32.

HENRICI, P. 1986 *Applied and Computational Complex Analysis*, Vol. 3. John Wiley.

HOWELL, L. H. & TREFETHEN, L. N. 1990 A modified Schwarz–Christoffel transformation for elongated regions. *SIAM J. Sci. Statist. Comput.* **11**, 928–949.

KOHLER, W. 1977 Power reflection at the input of a randomly perturbed rectangular waveguide. *SIAM J. Appl. Maths* **32**, 521–533.

LONG, R. B. 1973 Scattering of surface waves by an irregular bottom. *J. Geophys. Res.* **78**, 7861–7870.

MEI, C. C. 1983 *The Applied Dynamics of Ocean Surface Waves*. John Wiley.

MYSAK, L. A. 1978 Wave propagation in random media, with ocean applications. *Rev. Geophys. Space Phys.* **16**, 233–261.

NACHBIN, A. 1993 *Modelling of Water Waves in Shallow Channels*. Computational Mechanics Publicactions, Southampton, UK.

NACHBIN, A. & PAPANICOLAOU, G. C. 1992*a* Boundary element method for the long-time water wave propagation over rapidly varying bottom topography. *Intl J. Num. Meth. Fluids* **14**, 1347–1365.

NACHBIN, A. & PAPANICOLAOU, G. C. 1992*b* Water waves in shallow channels of rapidly varying depth. *J. Fluid Mech.* **241**, 311–332.

O'DONNEL, S. & ROHKLIN, V. 1989 A fast algorithm for the numerical evaluation of conformal mappings. *SIAM J. Sci. Statist. Comput.* **10**, 475–487.

O'HARE, T. J. & DAVIES, A. G. 1990 A laboratory study of sandbar evolution. *J. Coastal Res.* **6**, 531–544.

PAPANICOLAOU, G. C. & KELLER, J. B. 1971 Stochastic differential equations with applications to random harmonic oscillators and wave propagation in random media. *SIAM J. Appl. Maths* **21**, 287–305.

REY, V., BELZONS, M. & GUAZZELLI, E. 1992 Propagation of surface gravity waves over a rectangular submerged bar. *J. Fluid Mech.* **235**, 453–479.

ROSALES, R. R. & PAPANICOLAOU, G. C. 1983 Gravity waves in a channel with a rough bottom. *Stud. Appl. Maths* **68**, 89–102.

SRIDHAR, K. P. & DAVIES, R. T. 1985 A Schwarz–Christoffel method for generating two-dimensional flow grids. *Trans. ASME* I: *J. Fluids Engng* **107**, 330–337.

WHITHAM, G. B. 1974 *Linear and Nonlinear Waves*. John Wiley.